

# Assessing Quantitative Precipitation Estimation Methods Based on the Fusion of Weather Radar and Rain-Gauge Data

Alessio Biondi<sup>1</sup>, Graduate Student Member, IEEE, Luca Facheris<sup>2</sup>, Fabrizio Argenti<sup>3</sup>, Senior Member, IEEE, Fabrizio Cuccoli<sup>4</sup>, Senior Member, IEEE, Andrea Antonini<sup>5</sup>, and Samantha Melani<sup>6</sup>

**Abstract**—Accurate quantitative precipitation estimation (QPE) methods are essential for weather forecasting and for prevention of hydrogeological risk. QPE becomes even more important when facing severe precipitation events. In this letter, a comparison among different rainfall estimation methods is presented, using a severe event that occurred in Italy as a case study. In particular, the focus is on a merging method based on the dynamic adaptation of the  $Z$ - $R$  relationship according to the spatiotemporal evolution of the observed phenomenon. Through a cross-validation analysis, we quantitatively assess the effectiveness of such a method: compared with the others, it performs better on the average, while it can outperform them in critical rainfall conditions, confirming its potential for localizing and monitoring areas with greatest risks.

**Index Terms**—Merging methods, quantitative precipitation estimation (QPE), rain gauge, rainfall estimation, weather radar.

## I. INTRODUCTION

ESTIMATING rainfall at ground is important in a large number of meteorological and hydrological applications; it is also one of the main input parameters of early warning systems, which are crucial to face severe rainfall events. In such a context, accurate quantitative precipitation estimation (QPE) methods are indispensable as well as approaches able to provide a correct and detailed spatial retrieval of the rainfall fields.

Rain gauges and weather radars are the most employed instruments to monitor rainfall. Rain gauges provide point measurements of the amount of water fallen at ground in a given time interval. They are direct and accurate—so that they can be considered as a “ground-truth” reference—even though

they are typically sparse in space. The spatial representation of the whole rainfall phenomenon can be obtained only through interpolation techniques as, for instance, ordinary kriging (OK) [1]; thus, critical rainfall events featuring intense and persistent peaks may remain undetected if they are not sufficiently close to the nodes of the rain-gauge network. Weather radars are by far the most important instruments to observe precipitation at mesoscale, providing a spatially detailed map of precipitation. However, rainfall estimates are obtained indirectly from measurements made aloft of the power backscattered by raindrops [2], so that they may be quantitatively inaccurate.

For the above reasons, radar rainfall estimates and rain-gauge measurements exhibit complementary features, which need to be integrated. Radar rainfall estimates are obtained through the so-called  $Z$ - $R$  power-law relationships [3], which convert the radar reflectivity  $Z$  (in  $\text{mm}^6 \text{m}^{-3}$ ) into rainfall rate  $R$  (in  $\text{mm h}^{-1}$ ). A major problem is choosing the appropriate coefficients of the  $Z$ - $R$  relationship, as for a given value of  $Z$ , different choices of the coefficients may lead to huge differences in  $R$  [4]; due to the high variability of the raindrop size distribution, even during a single event, these coefficients vary both in time and space [5]. Therefore, from a QPE perspective, using a constant and a priori-selected  $Z$ - $R$  relationship—such as the well-known Marshall–Palmer (MP) [6]—is not the most suitable solution.

Merging the information provided by weather radars and rain-gauge networks to improve QPE has been investigated for several years (see, for instance, the review in [7]). The main differences among such approaches concern the weight they give to the information coming from rain gauges and radar. Geostatistical methods are based on the interpolation of rain-gauge measurements and exploit radars as ancillary providers of spatial information. Among such methods, we recall some derivations of the OK method, such as the kriging with external drift (KED) [8], and the conditional merging or kriging with radar-based error (KRE) correction [9]. Other approaches, for instance, the Brandes spatial adjustment (BSA) method [10], adjust radar rainfall estimates by introducing a correction term (either multiplicative or additive) obtained from rain-gauge measurements. Another class of methods uses an adaptive estimation of the coefficients of the  $Z$ - $R$  relationship so as to account for its variability in time and space [11]; this class includes the method presented by Cuccoli [12]

Manuscript received 5 June 2024; revised 11 July 2024; accepted 16 July 2024. Date of publication 29 July 2024; date of current version 7 August 2024. (Corresponding author: Luca Facheris.)

Alessio Biondi, Luca Facheris, and Fabrizio Argenti are with the Department of Information Engineering, University of Florence, 50139 Florence, Italy (e-mail: alessio.biondi@unifi.it; luca.facheris@unifi.it; fabrizio.argenti@unifi.it).

Fabrizio Cuccoli is with the Radar and Surveillance Systems (RaSS) Laboratory, Interuniversity National Consortium for Telecommunications (CNIT), 56124 Pisa, Italy (e-mail: fabrizio.cuccoli@cnit.it).

Andrea Antonini is with the Environmental Modeling and Monitoring Laboratory for Sustainable Development (Consorzio LaMMA), 50019 Sesto Fiorentino, Italy (e-mail: antonini@lamma.toscana.it).

Samantha Melani is with the Institute for the BioEconomy, National Research Council, 50019 Sesto Fiorentino, Italy, and also with the Consorzio LaMMA, 50019 Sesto Fiorentino, Italy (e-mail: melani@lamma.toscana.it).

Digital Object Identifier 10.1109/LGRS.2024.3434650

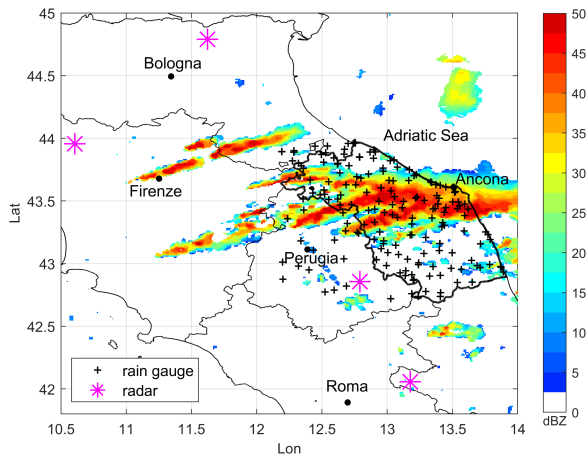


Fig. 1. CAPPI product at 2000-m height, 16:30 UTC, September 15, 2022. The black crosses and magenta asterisks mark the rain gauge and radar locations, respectively, while the black curves indicate the Italian regional borders.

and referred to as space–time adaptive coefficient conversion (STACC) in the following.

In this letter, we assess and compare the performance of different QPE methods, relying upon only the radar information (MP), only the rain-gauge network (OK), and on the fusion of the two data (KED, KRE, BSA, and STACC). Our performance analysis compares the different methods quantitatively, through a leave-one-out cross validation. Such a validation strategy also allows the robustness of each method to be assessed: in particular, we demonstrate that the STACC method outperforms the others in critical areas, i.e., in zones where the rainfall is high, but the rain-gauge deployment misses to sample the rainfall peaks. For the comparison, we used radar and rain-gauge data collected during a severe rainfall event occurred in 2022 in Italy.

## II. DATASETS AND METHODS

The radar and rain-gauge dataset used in this study refers to intense convective phenomena occurred on September 15, 2022, in central Italy, including V-shaped thunderstorms that remained over the Marche region for several hours due to the persistence of high- and low-pressure locations and to the presence of the mountain range of the Apennines that played a role of orographic triggering. As a result, dramatic levels of cumulated rainfall were recorded, in particular, from 15 to 18 UTC. Hail was not reported.

### A. Datasets

1) *Rain-Gauge Dataset*: The data come from a network consisting of 177 tipping bucket rain gauges, which provide rainfall measurements every 15 min in near real time. The position of each available rain gauge is shown in Fig. 1.

2) *Radar Dataset*: Weather radar data were collected by the Italian national weather radar network, which is managed by the Italian National Civil Protection Department (DPCN). This network covers the whole national territory and is made up of C-band radars, which perform synchronized scans every 5 min. The DPCN processes the raw data gathered by each

radar and then provides composite products on a national scale. The radar reflectivity used in this work is the constant altitude plan position indicator (CAPPI) product at 2000 m, which is available every 10 min. The chosen height is a good trade-off between the distance from ground (hence, from the rain-gauge network) and the need to avoid issues related to the local orography. Fig. 1 shows a sample of the CAPPI product provided by DPCN.

### B. STACC Method

Given a certain number of radar reflectivity (expressed in dBZ) maps available in a time interval  $T$  and considered a generic position  $(ln, lt)$  of the maps' grid expressed in longitude and latitude values, the algorithm computes  $Z_T(ln, lt)$  as the reflectivity averaged first over  $N_z$  neighboring positions in the grid and then over the time  $T$ . The time-averaged rainfall rate  $R_T(ln, lt)$  is then obtained through the model

$$\log_{10}(R_T(ln, lt)) = A_T(ln, lt) + B_T(ln, lt) \cdot Z_T(ln, lt) \quad (1)$$

where  $A_T(ln, lt)$  and  $B_T(ln, lt)$  are two space-varying coefficients that rule the conversion between reflectivity and rainfall rate. The quantities  $A_T(ln, lt)$  and  $B_T(ln, lt)$  are obtained with a two step procedure, calibration and interpolation, as follows. Consider a rain-gauge network composed of  $N_r$  elements, and let the position of the generic  $k$ th rain gauge be  $(ln_k, lt_k)$ ,  $k = 1, 2, \dots, N_r$ . Consider also a time interval  $T_w \leq T$ . Let  $ZW^{(k)}$  denote the radar reflectivity averaged in space (over an area centered on  $(ln_k, lt_k)$  and comprising  $N_z$  neighboring positions) and in time (over the interval  $T_w$ ), and let  $RW^{(k)}$  be the time-averaged (over the interval  $T_w$ ) rainfall rate measured by the  $k$ th rain gauge. Thereby, over the time interval  $T$  and for each rain gauge of the network, a set of couples  $(\log_{10}(RW^{(k)}), ZW^{(k)})$  is available, and, by using the model in (1), a linear regression yields the coefficients  $A_T(ln_k, lt_k)$  and  $B_T(ln_k, lt_k)$  related to the  $k$ th rain-gauge position  $(ln_k, lt_k)$ ,  $k = 1, 2, \dots, N_r$ . The coefficients  $A_T(ln, lt)$  and  $B_T(ln, lt)$  related to a generic grid position, i.e., different from those of the rain gauges, are calculated by means of spatial interpolation of the values  $A_T(ln_k, lt_k)$  and  $B_T(ln_k, lt_k)$ . The cumulated rainfall over the period  $T$ , at any grid position, is then given by

$$CR_T(ln, lt) = T \cdot R_T(ln, lt). \quad (2)$$

In summary, the algorithm provides a space-varying  $Z$ – $R$  relationship that is valid within a given time interval  $T$ . In particular, at each rain-gauge position, the coefficients of the  $Z$ – $R$  relationship are calibrated by using the data collected by the set of  $N_r$  rain gauges, whereas, at any other position, they are obtained by means of spatial interpolation.

1) *Implementation Details*: In the implementation of the STACC method, only a subset of the rain gauges has been used. During the calibration stage, rain-gauge data are considered “acceptable” if the values of  $A_T(ln_k, lt_k)$  and  $B_T(ln_k, lt_k)$ , obtained through linear regression as specified in Section II-B, fall within a reasonable range, as typically found in the literature [13]. Rain gauges for which this condition is not met are discarded and not used in the successive interpolation

stage. Specifically, we have used the weighted least square method described in [14], exploiting the temporal variability of radar and rain-gauge data as uncertainty parameter. As regards interpolation, the inverse distance weighting algorithm [15] has been employed.

### C. Other Methods for QPE

The STACC algorithm will be compared with other commonly used methods for QPE, which are here briefly reviewed along with some implementation details.

The MP  $Z$ - $R$  relation [6] uses only radar data to estimate rainfall rates. Since multiple radar reflectivity maps can be produced in the interval  $T$ , they are cumulated to achieve the final rainfall map. Using rain-gauge data only is possible by means of interpolation, for example, the OK algorithm. In this study, we employed, for OK, the open source library `GSTools` [16] setting the spherical model for fitting the empirical variogram (this setting was also used for the KED and KRE methods described below). The KED method [8] uses kriging interpolation with weights derived from a radar-based rainfall field estimate; in this study, the latter was achieved with the MP method. The BSA method [10] applies to the MP map a spatially varying multiplicative correction derived from the comparison with rain-gauge data. Specifically, we followed the procedure detailed in [17]. Not all the available rain gauges were used: in practice, rain gauges that either recorded less than 1 mm over the interval  $T$  or were located in positions where the MP estimate is less than 1 mm were discarded. The KRE correction method [9] adds a correction field to that estimated through OK. The error field is estimated by the following: 1) applying OK to the MP estimates at each rain-gauge position and 2) subtracting such a map to the complete MP map.

## III. EXPERIMENTAL RESULTS

This section is devoted to the comparison among the STACC method and other ones for estimating the cumulated rainfall maps. The comparative analysis is carried out using data relative to the time interval during which rainfall was extremely intense and caused severe damages. We also highlight a situation in which STACC outperforms the other methods (specifically, when there are no rain gauges sufficiently close to the position of local rainfall peaks) and discuss reasons of this behavior.

### A. Quantitative Analysis: Cross Validation

In order to evaluate the different rainfall retrieval algorithms from a quantitative point of view, a leave-one-out cross validation has been carried out. The procedure consists of the following: 1) leave one rain gauge out of the set of  $N_g$  available rain gauges; 2) estimate the cumulated rainfall map by using one of the methods to be compared; 3) evaluate the error between the estimate in the location of the left-out rain gauge and the true value recorded by it (ground truth); and 4) repeat the leave-one-out estimation for every rain gauge.

Let  $T_o$  be the total observation time during which the event is analyzed. Let us also assume that the cross-validation error

is computed with a time step  $T_s$ , chosen as a submultiple of  $T_o$ , so that we get  $N_t = (T_o/T_s)$  error samples at any rain-gauge position. In this manner, we obtain an  $N_g \times N_t$  matrix  $\Delta$ , whose generic element  $\Delta_{i,j}$  represents the error related to the  $i$ th rain gauge of the set at the  $j$ th time step  $T_s$ , that is,

$$\Delta_{i,j} = \Gamma_{i,j} - G_{i,j} \quad (3)$$

where  $G$  is the ground truth and  $\Gamma$  is its estimate. Only the rain gauges that have recorded at least 1 mm  $\text{h}^{-1}$  over  $T_o$  have been accounted for.

The accuracy of the estimation, and thus the performance of the different methods, is evaluated by using the mean absolute error (MAE) and the root-mean-square error (RMSE), defined as follows:

$$\text{MAE} = \frac{1}{N_t \cdot N_g} \sum_{j=0}^{N_t-1} \sum_{i=0}^{N_g-1} |\Delta_{i,j}| \quad (4)$$

$$\text{RMSE} = \sqrt{\frac{1}{N_t \cdot N_g} \sum_{j=0}^{N_t-1} \sum_{i=0}^{N_g-1} \Delta_{i,j}^2} \quad (5)$$

Table I shows the cross-validation results, for  $T_o = 180$  min and  $T_s = 30$  min, for all the considered methods. As expected, the improvements achieved by STACC (with  $T_w = 30$  min), KED, KRE, and BSA, with respect to methods based on either only radar data (MP) or only rain-gauge data (OK), are quite remarkable. For instance, comparing the STACC method with MP and OK, MAE improves of about 21% and 27%, respectively; in terms of RMSE, the percent reduction is 26% and 22%, respectively. On the other hand, the algorithms based on merging radar and rain-gauge information show similar performance indexes; the proposed STACC method, however, provides the best results in terms of all of them.

Based on the matrix  $\Delta$ , we can compute the performance indexes over longer time intervals. Consider overlapping time periods  $T_j = [jT_s, (j+k)T_s]$ , having a duration  $T'_s = kT_s$ , with  $k$  an integer, such that  $2 \leq k \leq N_t$ , and  $j = 0, 1, \dots, (N_t - k)$ . It is apparent that each interval  $T_j$  is characterized, with respect to  $T_{j+1}$ , by a time-shift and an overlap equal to  $T_s$  and  $(k-1)T_s$ , respectively. Let  $\Delta^{(k)}$  be the matrix whose entries are defined by

$$\Delta_{i,j}^{(k)} = \sum_{r=j}^{j+k} \Delta_{i,r} \quad (6)$$

where  $i = 0, 1, \dots, N_g - 1$  is the index spanning the rain-gauges set. In other words, the matrix  $\Delta^{(k)}$  contains the rainfall errors cumulated over a time interval  $T'_s$ , for each rain gauge; notice that it has the same number of rows ( $N_g$ ) of  $\Delta$  and a smaller number of columns ( $N'_t = N_t - k$ ). The definition of  $\Delta^{(k)}$  allows the performance indexes to be computed on the intervals  $T_j$ : it is sufficient to replace  $\Delta_{i,j}$  with  $\Delta_{i,j}^{(k)}$  and  $N_t$  with  $N'_t$  in (4) and (5).

The cross-validation results obtained for  $T'_s = 60$  min ( $k = 2$ ) and  $T'_s = 90$  min ( $k = 3$ ) are shown in Table I. In both cases, the STACC method exhibits the best performance, even though, also in this case, the differences with respect to the other methods based on the integration of rain gauge and radar information are not remarkable. Significant improvements,

TABLE I  
CROSS-VALIDATION RESULTS,  $T_o = 180$  min (FROM 15:00 TO 18:00 UTC)

Method	$T_s = 30$ min		$T'_s = 60$ min ( $k = 2$ )		$T'_s = 90$ min ( $k = 3$ )	
	MAE (mm)	RMSE (mm)	MAE (mm)	RMSE (mm)	MAE (mm)	RMSE (mm)
MP	4.55	8.93	8.85	16.63	13.25	24.38
OK	4.95	8.46	8.26	13.90	10.98	18.62
STACC	3.60	6.61	5.75	10.19	7.96	13.81
KED	3.83	6.80	6.27	10.28	8.57	14.06
KRE	4.00	7.04	6.59	11.13	8.57	14.77
BSA	3.74	6.66	6.51	10.41	9.16	14.27

TABLE II

ESTIMATION ERRORS RELATIVE TO THE CRITICAL CASE WHEN  $RG_A$  IS EXCLUDED FOR PREDICTION  $T = 60$  min (FROM 20:00 TO 21:00 UTC)

Method	$\Gamma_A$ (mm)	$\Delta_A$ (mm)
MP	47.78	-36.02
OK	10.70	-73.10
STACC	79.16	-4.64
KED	62.27	-21.53
KRE	47.50	-36.30
BSA	57.32	-26.48

instead, are reported with respect to MP (in particular) and OK, with increasing performance gaps as  $k$  increases: for instance, comparing the STACC results with those obtained by MP for  $k = 3$ , we get an improvement of 40% and 43% in terms of MAE and RMSE, respectively; compared with OK, MAE and RMSE are 27% and 26% smaller, respectively.

### B. Cross Validation: Discussion of a Critical Case

Detecting areas of very intense rainfall is of major interest. The absence of rain gauges nearby such areas may induce inaccurate rainfall estimates and, in this case, weather radar information becomes fundamental. In the following, we compare the behavior of the QPE methods previously analyzed in these “critical” situations.

Consider Fig. 2, which shows the averaged radar reflectivity over  $T = 60$  min (from 20:00 to 21:00 UTC). The rain gauge marked with “A” ( $RG_A$  in the following) is the only one within the area of maximum reflectivity. Removing  $RG_A$  from the available rain gauges allows the aforementioned critical cases to be simulated. As in the leave-one-out procedure, we assumed that  $RG_A$  is absent, applied the various rainfall estimation methods, and evaluated the error  $\Delta_A = \Gamma_A - G_A$ , between the cumulated rainfall  $\Gamma_A$  estimated in the position of  $RG_A$  and the rainfall  $G_A$  (ground truth) measured by  $RG_A$  itself. In the considered time interval  $T$ ,  $G_A$  is 83.80 mm. Table II shows the results for each estimation method.

Due to the lack of spatial details, the OK estimate is affected by a huge error, thus confirming the fact that the spatial information provided by radar data is fundamental. Such an error is so large that it has a remarkable impact also on the KRE estimate, which is based on corrections applied on

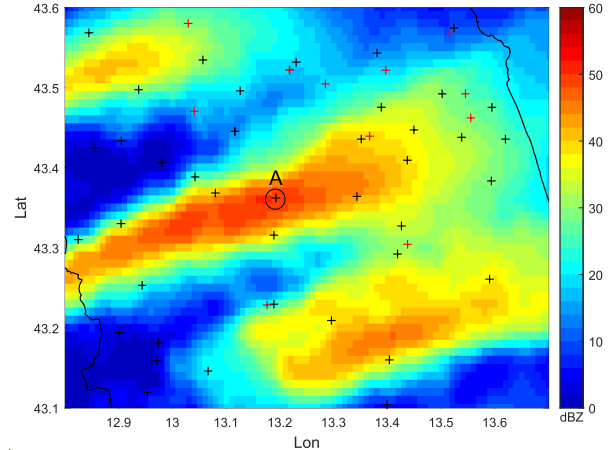


Fig. 2. Average radar reflectivity  $Z_T(ln, lt)$  from 20:00 to 21:00 UTC of September 15, 2022. “A” marks the rain gauge considered in the critical case analysis.

the OK map. As to the MP method, it is well known that it produces high errors in correspondence to high values of  $Z$  [18], and this fact is confirmed by the result in Table II. The issues of the MP method are inherited by the BSA approach. In fact, since  $RG_A$  is located where the reflectivity is high, the correction factor should be strong as well; however, when  $RG_A$  is dropped, the correction factor in that position—derived from the interpolation of small correction factors of the surrounding rain gauges—is underestimated. Note that also the KED estimate is rather poor: this is due to the fact that the weight given to the rain-gauge information is prevailing with respect to that given to the radar information.

Table II demonstrates that the STACC method yields the best performance among all the tested algorithms. In other terms, STACC is characterized by the smallest sensitivity to the removal of the critical rain gauge  $RG_A$ . What happens can be explained as follows. Once  $RG_A$  is dropped, only the surrounding rain gauges remain to generate the local  $Z-R$  relation, whose coefficients are then spatially interpolated: even though they are based on smaller values of  $R$  and  $Z$ , they are anyhow well representative of the link existing at higher levels of reflectivity and rainfall intensity.

For completeness, Fig. 3 shows the cumulated (over  $T$ ) rainfall maps obtained with each of the tested methods when the rain gauge  $RG_A$  is dropped.

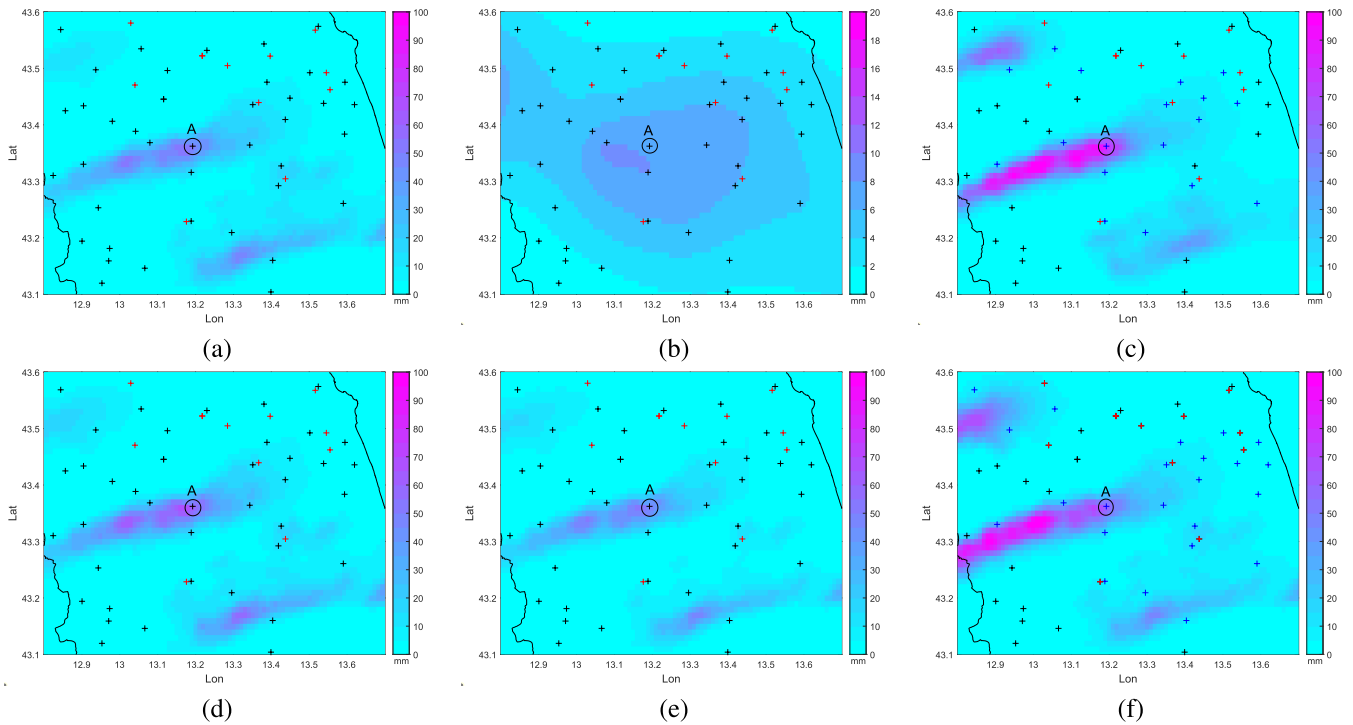


Fig. 3. Cumulated rainfall from 20:00 to 21:00 UTC on September 15, 2022, obtained by removing rain gauge  $RG_A$  (circled and marked with the letter “A” in the maps) and by using (a) MP, (b) OK, (c) STACC, (d) KED, (e) KRE, and (f) BSA. Notice that, in the OK case, for the sake of a better visualization, a different scale has been used.

IV. CONCLUSION

In this letter, we have presented an in-depth quantitative analysis of several rainfall estimation methods. As a case study, we used the data collected during a severe rainfall event occurred in Italy. Our comparisons have shown that, as expected, integrating radar and rain-gauges information is crucial, and that the STACC approach performs better than the other methods. In particular, the STACC method is very effective when there are no rain gauges where rainfall is most intense. To verify this, we have simulated this situation by dropping the input from a rain gauge placed inside a critical area and evaluated the ability of the various methods to predict the actual amount of rainfall in that area. The STACC method outperformed the other ones, demonstrating in this way its effectiveness and robustness for QPE.

ACKNOWLEDGMENT

The authors are grateful to the DPCN for providing the radar data.

REFERENCES

[1] H. Wackernagel, *Multivariate Geostatistics: An Introduction With Applications*, 3rd ed., Heidelberg, Germany: Springer, 2003.  
 [2] R. J. Doviak and D. S. Zrnic, *Doppler Radar and Weather Observations*, 2nd ed., San Diego, CA, USA: Academic Press, 1993.  
 [3] J. W. Wilson and E. A. Brandes, “Radar measurement of rainfall—A summary,” *Bull. Amer. Meteorological Soc.*, vol. 60, no. 9, pp. 1048–1060, Sep. 1979.  
 [4] D. Atlas, C. W. Ulbrich, and R. Meneghini, “The multiparameter remote measurement of rainfall,” *Radio Sci.*, vol. 19, no. 1, pp. 3–22, Jan. 1984.  
 [5] B. Chapon, G. Delrieu, M. Gosset, and B. Boudevillain, “Variability of rain drop size distribution and its effect on the Z–R relationship: A case study for intense Mediterranean rainfall,” *Atmos. Res.*, vol. 87, no. 1, pp. 52–65, Jan. 2008.

[6] J. Marshall, W. Hitschfeld, and K. Gunn, “Advances in radar weather,” *Adv. Geophys.*, vol. 2, pp. 1–56, Jan. 1955.  
 [7] S. Ochoa-Rodriguez, L. P. Wang, P. Willems, and C. Onof, “A review of radar-rain gauge data merging methods and their potential for urban hydrological applications,” *Water Resour. Res.*, vol. 55, no. 8, pp. 6356–6391, Aug. 2019.  
 [8] U. Haberlandt, “Geostatistical interpolation of hourly precipitation from rain gauges and radar for a large-scale extreme rainfall event,” *J. Hydrol.*, vol. 332, nos. 1–2, pp. 144–157, Jan. 2007.  
 [9] S. Sinclair and G. Pegram, “Combining radar and rain gauge rainfall estimates using conditional merging,” *Atmos. Sci. Lett.*, vol. 6, no. 1, pp. 19–22, Jan. 2005.  
 [10] E. A. Brandes, “Optimizing rainfall estimates with the aid of radar,” *J. Appl. Meteorol.*, vol. 14, no. 7, pp. 1339–1345, Oct. 1975.  
 [11] A. Libertino, P. Allamano, P. Claps, R. Cremonini, and F. Laio, “Radar estimation of intense rainfall rates through adaptive calibration of the Z–R relation,” *Atmosphere*, vol. 6, no. 10, pp. 1559–1577, Oct. 2015.  
 [12] F. Cuccoli, L. Facheris, A. Antonini, S. Melani, and L. Baldini, “Weather radar and rain-gauge data fusion for quantitative precipitation estimation: Two case studies,” *IEEE Trans. Geosci. Remote Sens.*, vol. 58, no. 9, pp. 6639–6649, Sep. 2020.  
 [13] M. Ignaccolo and C. De Michele, “One, no one, and one hundred thousand: The paradigm of the Z–R relationship,” *J. Hydrometeorol.*, vol. 21, no. 6, pp. 1161–1169, Jun. 2020.  
 [14] J. Orear, “Least squares when both variables have uncertainties,” *Amer. J. Phys.*, vol. 50, no. 10, pp. 912–916, Oct. 1982.  
 [15] B. Ahrens, “Distance in spatial interpolation of daily rain gauge data,” *Hydrol. Earth Syst. Sci.*, vol. 10, no. 2, pp. 197–208, Apr. 2006.  
 [16] S. Müller, L. Schüler, A. Zech, and F. Heße, “GSTools v1.3: A toolbox for geostatistical modelling in Python,” *Geoscientific Model Develop.*, vol. 15, no. 7, pp. 3161–3182, Apr. 2022.  
 [17] E. Goudenhoofd and L. Delobbe, “Evaluation of radar-gauge merging methods for quantitative precipitation estimates,” *Hydrol. Earth Syst. Sci.*, vol. 13, no. 2, pp. 195–203, Feb. 2009.  
 [18] G. Villarini and W. F. Krajewski, “Review of the different sources of uncertainty in single polarization radar-based estimates of rainfall,” *Surv. Geophys.*, vol. 31, no. 1, pp. 107–129, Jan. 2010.